Insect Biochemistry and Molecular Biology 118 (2020) 103312

Contents lists available at ScienceDirect

Insect Biochemistry and Molecular Biology

journal homepage: www.elsevier.com/locate/ibmb

The olfactory reception of acetic acid and ionotropic receptors in the Oriental armyworm, *Mythimna separata* Walker

Rui Tang[a], Nan-Ji Jiang[a,b], Chao Ning[a,b], Guo-Cheng Li[a,b], Ling-Qiao Huang[a], Chen-Zhu Wang[a,b,*]

[a] State Key Laboratory of Integrated Management of Pest Insects and Rodents, Institute of Zoology, Chinese Academy of Sciences, Beijing, PR China
[b] CAS Center for Excellence in Biotic Interactions, University of Chinese Academy of Sciences, Beijing, PR China

ARTICLE INFO

Keywords:
Mythimna separata
Acetic acid preference
Olfactory sensilla
Antennal lobes
Glomerulus
Ionotropic receptor

ABSTRACT

Various insect species including moths have shown significant foraging preference to acetic acid. However, the olfactory reception and behavioral outputs of acetic acid in moths remain unsolved. The female adults of Oriental armyworm, *Mythimna separata*, exhibit high preference to acetic acid enriched sweet vinegar solutions, making them good targets for exploration of acid reception and performance. We first proved that acetic acid is an essential component which elicited electrophysiological responses from volatiles of the sweet vinegar solution. Successive single sensillum recording tests showed that at least 4 types (as1, as2, as3, and as4) of sensilla were involved in acetic acid reception in the antennae. The low dosages of acetic acid elicited upwind flight and close search, and pre-contact proboscis extension responses of the fasted females, indicating it serves as a food related olfactory cue. *In vivo* optical imaging data showed that low dosages of acetic acid activated one ordinary glomerulus (DC3), and high dosages evoked additional two glomeruli (DC1 and AC1) in the antennal lobe. A systematic survey on olfaction related receptors in three related transcriptomes has yielded 67 olfactory receptors (ORs) and 19 ionotropic receptors (IRs). Among, MsepIR8a, MsepIR64a, MsepIR75q1, and MsepIR75q2 were chosen as putative acid receptors by blasting against known acid IRs in *Drosophila* and comparing essential amino acid residues which related to acid sensing. Later *in situ* hybridization revealed that *MsepIr8a* was co-expressed with each of the other 3 *Irs*, suggesting its putative co-receptor role. This study reveals olfactory reception of acetic acid as an attractant in *M. separata*, and it provides the solid basis for later deorphanization of relevant receptors.

1. Introduction

Insects precisely develop and possess a complex chemosensory system to communicate with the environment for survival (Joseph and Carlson, 2015). Olfaction is critical to this system and it conveys initial information in response to multiple chemical cues, including pheromones, host volatiles, or enemy smells (Allmann et al., 2013; Dweck et al., 2015; Ebrahim et al., 2015). Many of these compounds are acids, which exist widely in nature as common products of plants (Penniston et al., 2008; Zhu et al., 2003). To various insect species including armyworms, the odor of acetic acid can mean food signal, and they can be trapped by acetic acid-containing lures (Chiu, 1982; Cha et al., 2012; Landolt and Zhang, 2016; Meagher and Mislevy, 2005; Toth et al., 2010). Despite of agronomy practices which utilize acetic acid containing lures for monitoring and trapping of pest insects over decades, we have relatively limited knowledge on how acids were processed in the peripheral olfactory system.

Recent breakthroughs have been done in a model species, the vinegar fly *Drosophila melanogaster*, who uses acetic acid as an olfactory as well as a gustatory signal to assess food, oviposition medium, and mates (Chen and Amrein, 2017; Gorter et al., 2016; Gou et al., 2014; Joseph et al., 2009; Rimal et al., 2019). Acidity components are sensed through olfactory receptor neurons (ORNs) on the antennae, and they express a sophisticated receptor family called the ionotropic receptors (*Irs*), which, further divide into the antennal *Irs* that exist broadly among insects and species specific *Irs* (Abuin et al., 2011; Ai et al., 2010; Benton et al., 2009). *Irs* were reported in variant sensory pathways of *Drosophila* including olfaction (Ai et al., 2013; Prieto-Godino et al., 2017), gustation (Ahn et al., 2017; Ganguly et al., 2017; Hussain et al., 2016; Koh et al., 2014; Lee et al., 2018; Rimal et al., 2019; Sánchez-Alcañiz et al., 2018), thermosensation (Ni et al., 2016), and hygrosensation (Enjin et al., 2016; Knecht et al., 2016). In olfaction, detection

* Corresponding author. State Key Laboratory of Integrated Management of Pest Insects and Rodents, Institute of Zoology, Chinese Academy of Sciences, Beijing, PR China.
E-mail address: czwang@ioz.ac.cn (C.-Z. Wang).

https://doi.org/10.1016/j.ibmb.2019.103312
Received 21 July 2019; Received in revised form 25 December 2019; Accepted 27 December 2019
Available online 02 January 2020

of acetic acid involves a number of IRs, indicating that the acid sensing process is somewhat complicated in insects. In antennae of *D. melanogaster*, the sensilla coeloconica on the third chamber of the sacculus express one dedicated *Ir64a*, which mediates repellency toward high acidity stimuli (Ai et al., 2010). *Ir64a* is expressed together with a co-receptor *Ir8a* and they together form a tetramer complex to perform as an acid sensing ion channel (Ai et al., 2013). Furthermore, *Ir75a* is also used by *D. melanogaster* and *D. sechellia* to smell acetic acid and propionic acid (Abuin et al., 2011; Prieto-Godino et al., 2016). *Ir25a* and *Ir76b* mediate oviposition preference in female vinegar flies by sensing acetic acid and citric acid through gustatory reception (Chen and Amrein, 2017). *Ir7a* was reported to have essential role for *Drosophila* to reject sour food through gustatory reception by discriminating acid composition (Rimal et al., 2019). On the other hand, some cellular based research works have revealed that different dosages of acidity volatiles may evoke distinct glomeruli in the antennal lobes of *Drosophila*, resulting in various behavioral outputs (Semmelhack and Wang, 2009).

The olfactory reception of acetic acid in other insect species remain elusive. It is reported that glomeruli-based coding for feeding behaviors in *Manduca sexta* is related to acid sensing (Bisch-Knaden et al., 2018). *Aedes aegypti* mosquitoes were found to employ *Ir8a* pathway for detection of acidic volatiles from human odors (Raji et al., 2019). A systematic investigation is needed in non-model insects, especially insect pests who employ acetic acid as a food related odorant (Faucher et al., 2013). The Oriental armyworm moth, *Mythimna separata* Walker (Lepidoptera: Noctuidae), also known as *Pseudaletia separata*, is a major pest of crops in Asia and it has been monitored with acetic acid riched lures for decades (Jiang et al., 2014). In particular, sweet vinegar solution luring is one of the most cost-effective methods for trapping this pest (Jiang et al., 2014). Due to the high proportion of acetic acid in its luring recipe, *M. separata* is a suitable target for exploring the olfactory basis on acetic acid attractiveness. Here, we integrate behavioral, electrophysiological, cellular, and molecular methods to investigate olfactory reception for acetic acid in *M. separata*. We examined the behavioral responses of the female adults, the electrophysiological responses in antennal sensilla, the calcium imaging activities in antennal lobes to acetic acid. We also annotated olfaction related receptor gene families from transcriptomes of antennae and pheromone gland-ovipositors (PGO) of *M. separata*. Finally, 4 putative acid sensing IRs were selected and characterized in terms of expression and localization patterns.

2. Materials and methods

2.1. Chemical analysis

All chemicals and reagents mentioned in this study can be found in Table S4. Tested sweet vinegar solution samples were made by mixing white wine and vinegar at a 1:3 ratio (Jiang et al., 2014). Samples were desiccated with calcium chloride drying agent columns and then analyzed with an Agilent Technologies 5973 mass spectrometer coupled with an Agilent Technologies 6890N gas chromatography system (Santa Clara, CA, USA) equipped with a quartz capillary column (HP-5, 30 m × 0.25 mm × 0.25 μm; J&W Scientific, Palo Alto, CA, USA). Volatile compounds were identified by crosschecking with the mass spectrum fragment database (NIST 2.0) with GC/MSD ChemStation (Agilent) and confirmed against standard chemical spectrum patterns. Three replicates were conducted for the sample solution blend.

2.2. Electroantennographic detection

GC-EAD system was used to screen for bioactive chemical compounds following standard protocols as described previously (Tang et al., 2016). Antennae were processed by cutting both extremes and immediately mounted with two glass capillary Ag/AgCl electrodes containing Kaissling saline (Tang et al., 2016) and an identical gas chromatography column was used under the same temperature program as for chemical analysis with the detector at 230 °C. The electrode at the distal end of the antenna was connected via an interface box to a signal acquisition interface board (IDAC; Syntech, Kirchzarten, Germany) connected to a computer. Electroantennogram signals and flame ionization detector responses from the gas chromatography were recorded simultaneously. Bioactive chemicals were identified by cross-checking with GC-MS data. At least 3 replicates were performed for each gender in each species.

Dose response curves were tested for acetic acid using concentration gradient water solutions. Five concentrations were used as treatments, including w/w 0.001%, 0.01%, 0.1%, 1% and 10% with water alone used as a blank control. Eleven replicates were tested for females and 18 replicates were tested for males with each treatment.

2.3. Wind tunnel assay

The wind tunnel experiments and data process methods were adopted from a previous study on lepidopterous insects in a dark room (Tang et al., 2012). One to 3 day newly emerged female *M. separata* moths were collected and blocked into two groups. One group was fed with enough 10% honey water and another group was fasted for over 12 h before the test. The wind tunnel flying section cubic area was 90 cm × 90 cm × 240 cm. Filtered air was provided through the tunnel inlet via a centrifugal fan at 10 cm/s. The outflowing air was collected by another fan and released through a sealed pipe into the atmosphere. The flight section was lit diffusely from above with red lights at 10 lux. The room temperature was kept at 23 ± 2 °C and 40–60% relative humidity. Experiments were conducted at the 4th to 8th hour of the dark phase. Tested chemical solutions include: (1) water, (2) 0.01% acetic acid, (3) 0.1% acetic acid, (4) 1% acetic acid, (5) 10% acetic acid, (6) 50% acetic acid, (7) 1% enanthic acid, and (8) the sweet vinegar solution containing 10% acetic acid. They were prepared on the day of testing and white filter paper loaded with 10 μl solutions were used as odorant sources. Olfactory stimuli were released from the center of the upwind end of the tunnel and moths were released from a metal mesh cage at the center of the downwind end. Behaviors were recorded for 5 min in terms of taking off, upwind flight, close search, and landing. Twenty-five (fed) and 35 (fasted) moth adults were used for each treatment, respectively.

2.4. The capillary feeding assay

The capillary feeding (CAFE) assay was carried out on 12 h fasted naive moth adults using plastic tubes (diameter = 2 cm, length = 10 cm) and meshed plugs. A capillary loaded with 50 μl tested solution was fixed with one tip in the center of the tube through the plug, and a small piece of filter paper was attached to the tip of the capillary to increase evaporation. The filter paper was previously soaked with the tested solution. The treatments and the number of tested moths were as follows: (1) water, n = 51; (2) 1% sucrose, n = 51; (3) 1% sucrose + 0.1% acetic acid, n = 35; (4) 1% sucrose + 1% acetic acid, n = 39; (5) 1% sucrose + 10% acetic acid, n = 32; (6) 0.1% acetic acid, n = 30; (7) 1% acetic acid, n = 52; (8) the sweet vinegar solution containing 1% acetic acid, n = 52. Successive behaviors of the introduced moth in 3 min were observed and recorded. The pre-feeding duration is defined as the time the moth spent to locate and feed on the solution. The percentage of feeding moths is the rate of tested moths with the continuous feeding behavior. The feeding amount is the total volume consumed by a single moth during the first meal, which was calculated according to the formula $x = L \times 50/L_0$ (μl), x indicates feeding volume; L indicates the consumed length; L_0 indicates the length of 50 μl solution. The percentage of proboscis extension response (PER) moths is the rate of tested moths showing PER. The percentage of pre-contact PER moths is the rate of

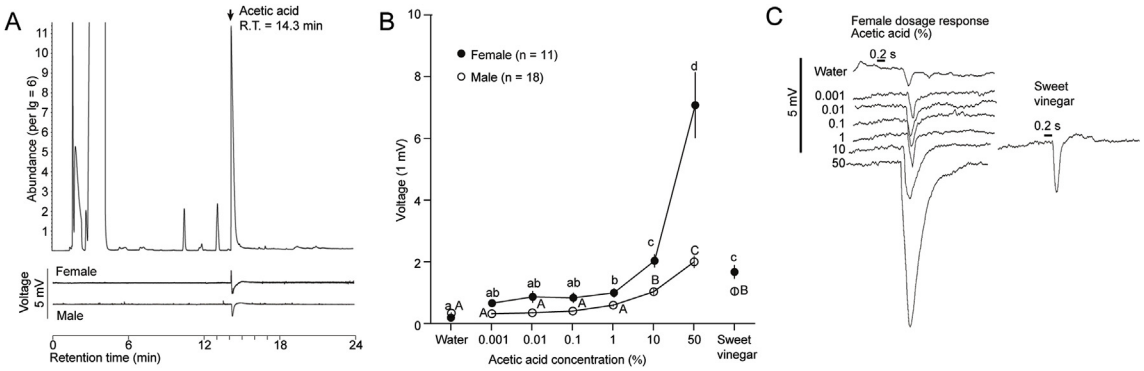

Fig. 1. Electrophysiological tests with *M. separata* antennae to sweet vinegar and laddered acetic acid solutions. (A) Example GC-EAD traces with antennae from female and male *M. separata* adults to sweet vinegar solution volatile blends. **(B)** Comparison of EAG responses with antennae of both genders of *M. separata* toward multiple tested solutions. Water was used as control. The sweet vinegar solution contained equivalent 10% acetic acid, the formula of the solution was shown in methods section. Example traces of female antennae were shown on the right. Different lower-case letters indicate significant different responses were stimulated among treatments in females (female: $F_{7,\ 172} = 63.6$, $P < 0.0001$). Different upper-case letters indicate significant different responses were stimulated among treatments in males ($F_{7,\ 138} = 28.0$, $P < 0.0001$). Error bars indicate ± s.e.m. **(C)** Example traces showing representative responses of the moth's antennae to all tested treatments.

tested moths showing PER before contacting the filter paper.

2.5. Single sensillum recording

Two to 3-day old moths were mounted with dental wax inside a 1 ml tip-cut Eppendorf tube and then fixed on a mounting block with the moth's antennae stretched out sensilla side up. The reference electrode was inserted into a compound eye, and the sharpened recording tungsten electrode was inserted into the base of a single sensillum in the front area of the antenna. Spike numbers in 1 s were calculated by 200 ms spikes timed 5 (Xu et al., 2016). Spike sorting and tempo distribution analysis were done referring to previously reported works on moths and vinegar flies (de Bruyne et al., 2001; Ghaninia et al., 2014). Thirty female adults were recorded and among, five separated sensilla in each segment from 3 moths were randomly sampled to investigate distributions of acid sensilla.

2.6. Antennal lobe calcium imaging

A single 2-3-day old *M. separata* adult was mounted in an artificial mounting block with its antennae being stretched out for chemical stimuli. After dissecting and exposing the brain, the antennal lobe was stained with a calcium-sensitive dye, Calcium Green and Pluronic F-127 mix for 1 h at 13 °C, and then thoroughly rinsed with Ringer solution. For imaging, we used a Till Photonics imaging system equipped with a CCD camera connected to an upright microscope. The antennal lobe was illuminated at 475 nm and odorant stimulation started at frame 13 and lasted 500 ms in the recording sequence of 40 frames. The tempo - fluorescence data was transferred and peak 2 to 3 reaction values were selected among frames 13 to 18 (Wu et al., 2015) for statistics. A total 8 moths were recorded for acid patterns, and 6 moths were recorded for acetic acid dosage responses.

2.7. Antennal lobe atlas

Brains of moths were dissected and processed according to published works (Zhao et al., 2016) and SYNORF1 (Developmental Studies Hybridoma Bank, IA, USA) antibody was used to label glomeruli in antennal lobes. Labelled antennal lobes were visualized with Alexa Fluor 488 goat anti-mouse secondary antibody (Invitrogen) and photo stacks were obtained with a Zeiss LSM710 Meta laser scanning microscope (Zeiss, Oberkochen, Germany). Atlas of *M. separata* brain was done using AMERA 6.0 software (ZIB, Germany). Seven female adults were tested.

2.8. Antennal transcriptome

According to a previous report (Ning et al., 2016) antennae of male and female *M. separata* moths were collected and stored at −80 °C for transcriptome sequencing. Total RNA was extracted using a RNeasy Mini Kit and reverse transcription of cDNA and Illumina library development were performed for Illumina HiSeq2500 sequencing at BGI Co., Beijing, China. High quality clean reads of nuclear sequences were obtained by removing adaptor sequences, empty reads and low-quality sequences (N > 10% sequences) and the reads with more than 50% Q < 20 base using FastQC tool. Clean reads data were combined and *de novo* assembled with Trinity (Haas et al., 2013). *Or* and *Ir* annotations were manually done against reported *IR* genes with BLAST. Protein structures of genes of interest were predicted with Swiss-model. Translated amino acid sequences were first aligned with ClustalW and phylogenetic tree was developed using the Neighbor-Joining method (Saitou and Nei, 1987) in MEGA 7.0.14 software (Kumar et al., 2016).

2.9. Reverse transcription PCR and verifications of Irs

Reverse transcription PCR was used to analyze tissue expression patterns of related *Irs* among *M. separata* male antennae (MA), male labial palp (ML), male proboscis (MP), male tarsi (MT), male wing (MW), female antennae (FA), female labial palp (FL), female proboscis (FP), female tarsi (FT), female wing (FW) and ovipositor (O). RT-PCR was done using a standard protocol with household gene *β-actin* as control to verify the experimental situation, and the primers were accepted until unified weight products were observed in electrophoresis. The full CDS primers were then used to obtain full length of each *Ir*. When full length was obtained, we then were able to confirm the existence of the corresponding genes. A total 3 technical replicates were done for RT-PCR tests. Primers used in the study were listed in Table S2.

2.10. Fluorescence in situ hybridization

Two-color *in situ* hybridization was performed as described previously (Ning et al., 2016). Probes of tested IRs were labelled with digoxin or biotin using an RNA labeling Kit version 12 (SP6/T7), with Dig-NTP or Bio-NTP labeling mixture, respectively. Visualization of hybridization signals was performed by successively incubating the sections with HNPP/Fast Red and Biotinyl Tyramide Working Solution with the TSA kit protocol. All sections were analyzed under Zeiss LSM710 microscope. A total 20 pairs of antennae were tested for each treatment.

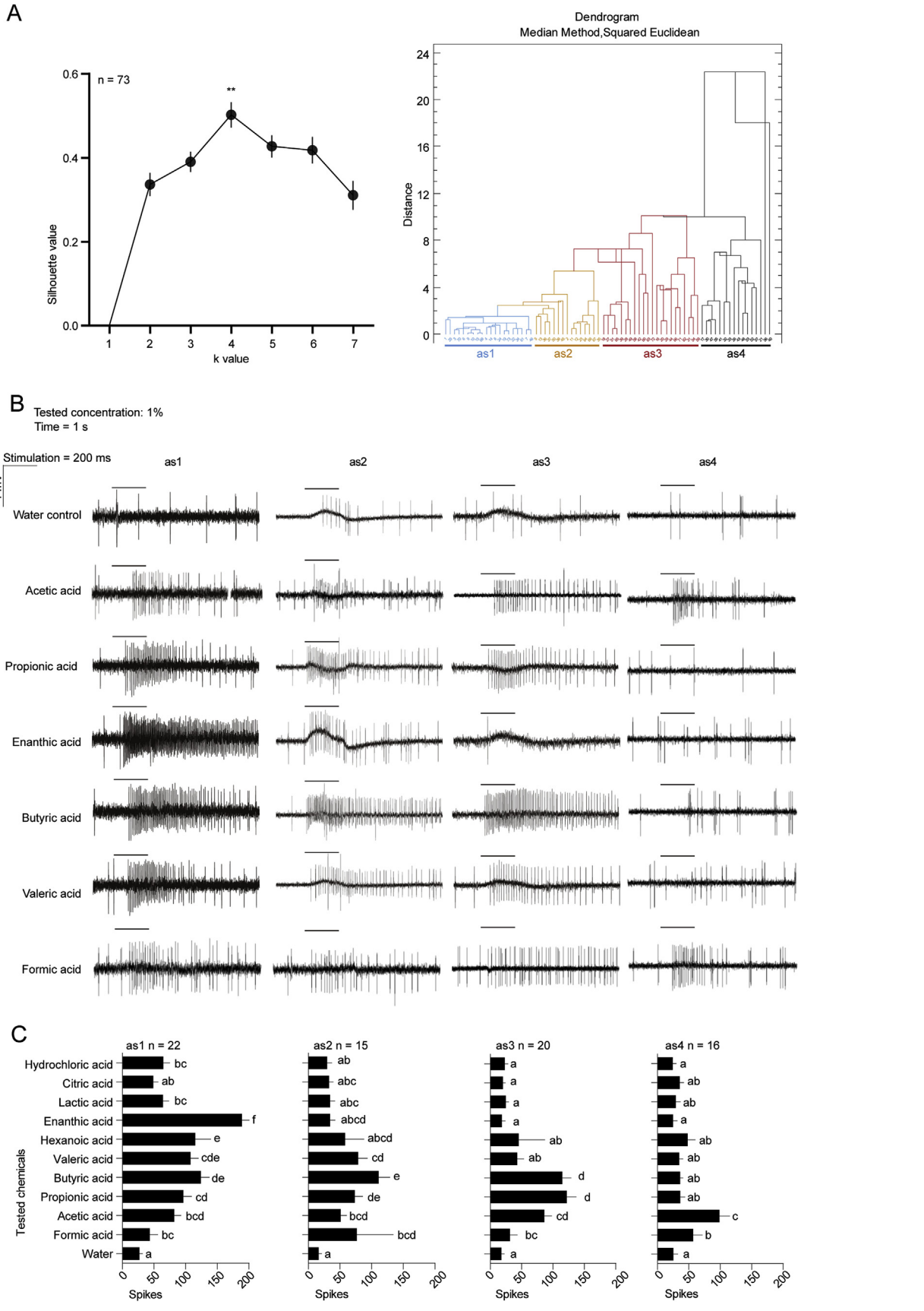

(caption on next page)

Fig. 2. Clustering and characterization of acetic acid active sensilla on female *M. separata* antennae with SSR tests. (A) Clustering of sensilla using silhouette method. The peak silhouette value at $k = 4$ was significantly different from other k values ($F_{6, 445} = 11.47$, $P < 0.0001$, n = 73). Dendrogram was developed from standardized values by Median Clustering Method and distance metric was calculated by Squared Euclidean. Clustering observations contain tested chemicals including water control, acetic acid, propionic acid, enanthic acid, butyric acid, valeric acid, lactic acid, citric acid, and hydrochloric acid. **(B)** Representative spike patterns of as1 (n = 22), as2 (n = 15), as3 (n = 20), and as4 (n = 16) type sensilla. All tested chemicals were applied at 1% concentration. Spikes within 1 s were shown. **(C)** Statistics of as1, as2, as3, and as4 sensilla. Bars with different lower-case letters indicate significant differences of spike counts among treatments in each type sensillum (*as*1: $F_{10, 199} = 34.3$, $P < 0.0001$; *as*2: $F_{10, 130} = 17.6$, $P < 0.0001$; *as*3: $F_{10, 177} = 54.8$, $P < 0.0001$; *as*4: $F_{10, 139} = 23.0$, $P < 0.0001$). Error bars indicate + s.e.m.

2.11. Data processing and statistical analysis

Statistics were carried out using IBM SPSS Statistics 22.0.0 (SPSS, Chicago, IL, USA). Comparison of means was done with one-way ANOVA, followed by Tukey HSD multiple comparison tests. Percentage data were compared with *Chi*-square test. Bar charts were plotted using Prism 5 for Windows ver. 5.01 (GraphPad software, San Diego, CA, USA). Correlation matrix was developed with Statgraphics Centurion XVII (Statpoint Technologies, Inc., VA, USA). Calcium imaging graphics and *k*-means clustering were processed with MATLAB 7.8.0.347 (The MathWorks, Natick, MA, USA).

2.12. Data availability

Gene deposition information for this study can be found in Table S3. Chemicals and reagents in this study have been listed in Table S4. Arithmetic for processing clustering and/or correlation are available upon request.

3. Results

3.1. Acetic acid from volatiles of sweet vinegar solution elicited significant electrophysiological responses in M. separata

The sweet vinegar solution has been recommended for control of *M. separata* in China back to 1980s (Chiu, 1982). To understand the role of acetic acid in the sweet vinegar solution, we first investigated the volatiles from this mixture through the Gas Chromatography coupled with Mass Spectroscopy (GC-MS). Among a total 12 identified chemicals, acetic acid was one of the major components (Table S1). In the Gas Chromatography coupled with Electroantennographic Detection (GC-EAD) tests, acetic acid evoked dramatic responses in several species including *M. separata* (Fig. 1A and Fig S1). In successive electroantennogram (EAG) tests, acetic acid was eliciting a moderate response comparing to other acids (Fig S2). Responses of *M. separata* were positively related to acetic acid dosages, and the sweet vinegar solution which contained equivalent 10% acetic acid has stimulated similar responses as acetic acid at the same concentration (Fig. 1B and C). Moreover, female adults were more sensitive to acetic acid than males (Fig. 1B), thus, only female moths were investigated in later tests.

3.2. At least four types of sensilla are involved in acetic acid sensing in M. separata

Next, we conducted single sensillum recording (SSR) tests to identify the sensilla responding to acids in *M. separata* (Fig S3). We have tested 30 female adults and identified 74 sensilla which had clear responses to acetic acid. Spike-count data from all acids were then transferred into *z*-scores and clustered according to the silhouette method at $k = 2$ to 7 (MacQueen, 1967; Prieto-Godino et al., 2016; Rousseeuw, 1987). The highest silhouette values of 4 indicated that the sensilla were most likely to be classified into 4 clusters (Fig. 2A and Fig. S4). We then named these four clusters as as1, as2, as3, and as4 type sensilla, respectively. Each single sensillum was assigned to the clusters with the Median Method clustering, which was further proved with a correlation matrix and manual correction (Fig. 2A and Fig. S4). The numbers of the four types of sensilla, as1, as2, as3, and as4 were 22, 15, 20, and 16, respectively.

The sensillar types as1, as2, and as3 were broadly tuned to several acids but with different sensitivities, while as4 was narrowly tuned to acetic and formic acids only. The as1 sensilla significantly responded to 9 out of 10 tested acids, and the response to enanthic acid was the highest with a tonic tempo distribution pattern (Fig S5). The as2 responded to 5 acids and the highest one was butyric acid. Both propionic acid and butyric acid sensilla elicited the highest responses of as3 (Fig. 2B and C). Sensilla as1, as2, and as3 responded to acetic acid with moderate responses compared with other acids, while as4 had the best response to acetic acid. For all sensilla types, significant responses could be observed when applied acetic acid at 1%, and an increase was found along with dosages (Fig. 3).

3.3. Acetic acid attracts M. separata in a dosage manner

We asked the behavioral outputs of acetic acid by comparing it to the sweet vinegar solution in the wind tunnel tests. Result showed that the sweet vinegar solution and 0.1%–10% acetic acids elicited comparable take-off, upwind flight, and close search behaviors to *M. separata*, excepted for landing behaviors (Fig. 4). Concentrations of 0.1%, 1%, and 10% acetic acids all caused significant upwind flights comparing to the water control, while an overwhelming concentration of 50% acetic acid did not elicit significant upwind flight (Fig. 4B). Moreover, 12 h fasted moths were more attracted by acetic acid than fed moths (Fig S6B). We next checked behavioral outputs of *M. separata* adults to enanthic acid, since enanthic acid induced the strongest electrophysiological response of as1 sensilla. On the contrary to its outstanding performances against as1 sensilla during SSR tests, enanthic acid at the concentration of 1% did not elicit significant upwind flight to *M. separata* (Fig. 4).

We then used a CAFE assay to test the behavioral responses of fasted moths to acetic acid in a short range (Fig. 5A and Movie 1). Results showed that acetic acid containing solutions significantly reduced the pre-feeding duration comparing with 1% sucrose alone (Fig. 5B). Percentages of feeding moths in 1% sucrose and sucrose-acid mixtures were significantly higher than that in water, and the mixture of 0.1% acetic acid and 1% sucrose had significantly higher feeding percentage than 1% sucrose alone (*Chi*-square test, $P = 0.044$). However, addition of 10% acetic acid remarkably inhibited feeding behaviors of the moths (Fig. 5C). 0.1% acetic acid along or mixed with 1% sucrose gained the largest feeding amount among all the tested solutions (Fig. 5D). The pre-contact PER was observed in acetic acid containing treatments but not in 1% sucrose (Movie S1), indicating that acetic acid as an olfactory cue could induce PER responses of moths (Fig. 5E and F).

Supplementary video related to this article can be found at https://doi.org/10.1016/j.ibmb.2019.103312.

3.4. DC3 glomerulus is exclusively evoked by acetic acid under attractive dosages

Next, we traced the acetic acid signaling in the antennal lobe, the first olfactory neuropil of the moth's brain. In *in vivo* optical imaging tests, a total three different regions of interest (ROIs) were evoked by different acids (Fig. 6A and Fig. S7A). Distinct patterns were evoked by

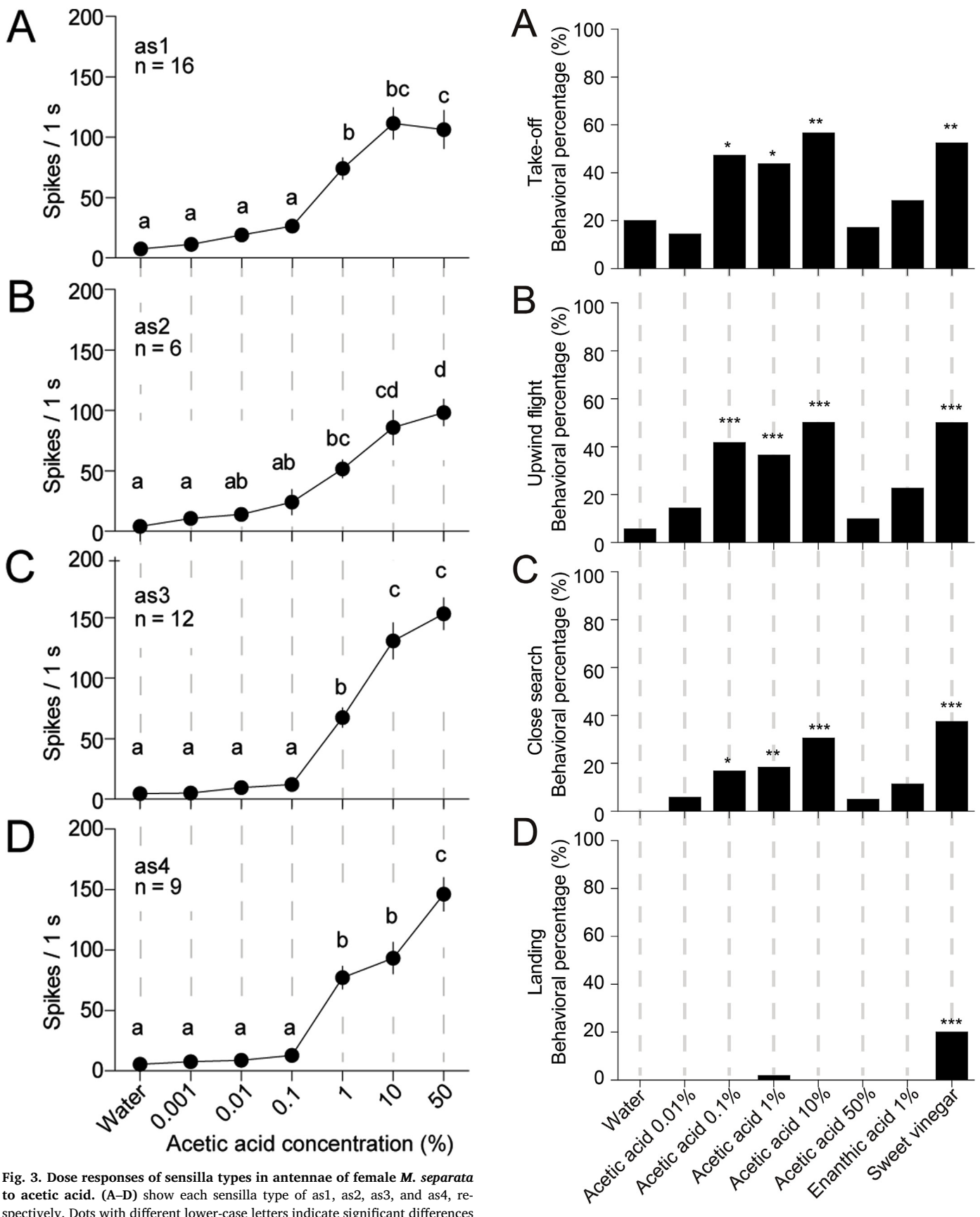

Fig. 3. Dose responses of sensilla types in antennae of female *M. separata* to acetic acid. (A–D) show each sensilla type of as1, as2, as3, and as4, respectively. Dots with different lower-case letters indicate significant differences of spike counts among dosages (as1: $F_{6,\ 104} = 28.4$, $P < 0.0001$; as2: $F_{6,\ 35} = 19.4$, $P < 0.0001$; as3: $F_{6,\ 77} = 60.4$, $P < 0.0001$; as4: $F_{6,\ 56} = 47.0$, $P < 0.0001$). Error bars indicate ± s.e.m.

(caption on next page)

Fig. 4. Behavioral responses of female *M. separata* to acidity solutions in wind tunnel. The sweet vinegar solution was used at equivalent concentration of 10% acetic acid. **(A–D)** Comparison of four attractiveness behaviors elicited by multiple acidity odorant sources in 12 h fasted female moths. Asterisks indicate significant higher percentages of the treatments comparing with water (*: $P < 0.05$, **: $P < 0.01$, ***: $P < 0.001$).

acetic acid stimuli: only 1 area (ROI2) was constantly evoked when tested from 0.1% to 10%, while 3 areas were evoked when applied at 50% (Movie S2). Enanthic acid evoked only 1 area with weak intensity regardless of dosages (Movie S3). Propionic acid, butyric acid, and valeric acid all evoked 3 areas (Fig S7A). The dose-response curve of acetic acid in ROI2 shows that the response started at 0.1% and it increased with dosages (Fig. 6B). Citric acid, lactic acid, or hydrochloric acid did not show a significant evoking pattern under the scope of this study (Fig S7B).

Supplementary data related to this article can be found at https://doi.org/10.1016/j.ibmb.2019.103312.

In order to identify correspondence glomeruli in the antennal lobe, we merged ROIs from the above 5 active acids. Result showed that the ROIs from all acids were highly overlapped, indicating 1 glomerulus was involved in each area (Fig. 7A). We later established 3-D structures of *M. separata* female antennal lobes with a standard atlas protocol (Berg et al., 2002; Lofaldli et al., 2010; Zhao et al., 2016), and then we compared the morphology of glomeruli with optical imaging results. The glomeruli which reflected ROIs were identical in terms of positions and volumes among individuals (Fig. 7 and Fig. S8). We then named them according to locations as DC1 (dorsal central 1), DC3, and AC1 (anterior central 1) glomerulus. As DC3 was the only one which was evoked under the attractiveness dosages of acetic acid, it is highly likely to be the glomerulus which was involved in acetic acid stimulated attractiveness.

3.5. Four IRs are identified as putative acetic acid receptors

Although results showed that acids can be sensed through the olfactory system in *M. separata*, the molecular basis is still to be explored. To this end, we annotated the major olfaction related receptor family genes from the transcriptome of female and male antennae, and PGO of *M. separata* adults, harvesting 67 *Ors* and 19 *Irs* (Fig. S9 and Fig. 8A, Tables S3 and S5). Although we cannot exclude possible role of ORs in sensing other bioactive volatile components from sweet vinegar blends, there is no evidence so far to support possible involvement of ORs in acid olfactory reception in any insects, so that we then emphasized on the *Ir* family genes. Among 19 *Irs*, *MsepIr8a*, *MsepIr25a* and *MsepIr76b* were highly expressed in the antennae of both genders of adults. Furthermore, *MsepIr25a* was also moderately expressed in PGO. Other left *Irs* were mostly expressed in antennae than PGO, excepted for *MsepIr10a* which had a reversed expression profile, and *MsepIr64a* which almost evenly expressed in all three tissues (Fig. 8B).

To narrow down target genes for acid sensing, we referred to already characterized acid sensing IRs in *D. melanogaster* (Abuin et al., 2011; Benton et al., 2009). In the phylogenetic analysis, two major clades were formed, namely the *Ir64* clade and the *Ir75* clade (Fig. 8A). For *M. separata*, an expansion of *Ir75* clade was observed, including 6 genes and covering 32% of the total number of IRs identified in the transcriptomes. On the other hand, only *MsepIr64a* was found in the corresponding clade. After verification by PCR tests (Materials and methods 2.9), we confirmed existences of 4 genes - *MsepIr8a*, *MsepIr75q1*, *MsepIr75q2*, and *MsepIr64a*. The tissue-gender expression levels of the 4 genes were similar with results from transcriptome analysis (Fig. 8C and Fig. S10).

Based on the structural prediction of IRs, MsepIR8a had a dimer structure while MsepIR64a, MsepIR75q1, and MsepIR75q2 were monomeric, which, was similar to the situation of the acid olfactory counterparts in *D. melanogaster* (Fig. S11). By comparing with structures of *Drosophila* IRs (Benton et al., 2009), we observed high conservation of IR8a and IR25a between the two species. MsepIR8a maintains the 3 key amino acid residues with DmelIR8a, while MsepIR25a does not. The 3 residues are R493 in the S1 region, D660 and I709 in the LBD (ligand binding domain) region (Fig. 8D). This implies that MsepIR8a could be functionally consistent with its ortholog in *Drosophila* as an acid sensing co-receptor.

When compared with ligand binding IRs in *Drosophila*, we also observed in *M. separata* a conserved arginine (R) residue in S1 region for MsepIR64a (R276), MsepIR75q1 (R286), and MsepIR75q2 (R293), suggesting their potential carboxyl binding activity (Fig. 8D). Meanwhile, MsepIR75q1 and MsepIR75q2 also maintain a key valine residue at V484 and V492 in the S2 region, respectively. This residue has shifted to I464 in MsepIR64a. So far, the key residues of above four IRs in *M. separata* were consistent with those IRs involved in acid sensing in *Drosophila*, suggesting that MsepIR8a, MsepIR64a, MsepIR75q1, and MsepIR75q2 could be selected as candidate IRs in later deorphanization of the acetic acid receptor(s) (Fig. 8D and Fig. S12).

3.6. Co-expression with selected Irs shows the co-receptor role of MsepIr8a

According to the tissue expression profile and structural prediction results, it is likely that *MsepIr8a* is the co-receptor gene for acid olfactory reception like in *Drosophila*. To investigate this, we carried out two-color fluorescence *in situ* hybridization with probes for these four genes. The results showed that *MsepIr64a*, *MsepIr75q1*, and *MsepIr75q2* were consistently co-expressed with *MsepIr8a* in the antennae of females (Fig. 9A, B, and C). Thus, there might be quite a few combinations of possible IR groups (IR8a/IR64a, IR8a/IR75q1, IR8a/IR75q2) in *M. separata* to fulfill acid olfactory reception. Furthermore, more expressed *MsepIr8a* can be observed without co-expression with either *MsepIr64a*, *MsepIr75q1*, or *MsepIr75q2*, suggesting *MsepIr8a* could be co-expressed with other ligand binding *Irs* in *M. separata* (Fig. S13).

4. Discussion

In the current study, we first proved that acetic acid is the major bioactive compound in the sweet vinegar solution attractive to *M. separata*. Acetic acid elicited upwind flight and close search, and pre-contact PER of the fasted female moths, indicating it serves as a food related olfactory cue, similar to that in *Drosophila* (Ko et al., 2015; Lebreton et al., 2012). However, 1% or higher acetic acid induces highly repulsive feeding responses of the moths, compared with sucrose alone. These results suggest that acetic acid works on the moths through two chemosensory modalities: olfaction induces attraction to make close search behavior, while gustation mediates repulsion to avoid sour food. The dual functions may have different emphasis during food/host selection as shown also in *Drosophila* species (Ai et al., 2010; Chen and Amrein, 2017; Rimal et al., 2019). Next, we found at least 4 types of acid sensing sensilla with different spectra including acetic acid. Later we located a dedicated glomerulus DC3 in the antennal lobe, which was the only glomerulus evoked by acetic acid at the attractive concentrations (0.1%–10%).

In the antennal lobe of *Drosophila*, IR- and OR-based neurons project to distinct glomeruli (Ai et al., 2010; Münch and Galizia, 2016). More importantly, the same IR expressed neurons from different sensilla types can project to the same glomerulus, as *DmelIr75d* is expressed in ORNs of both ac2 and ac4 sensilla and the neurons together project to VL1 glomerulus (Grabe et al., 2016). These results may also extrapolate to IR-based olfactory reception in *M. separata*. Given the fact that several types of sensilla can respond to the attractive dosages of acetic acid but only one glomerulus was evoked, we suggest that IR-based neurons sensitive to acetic acid from these sensilla project to DC3. To date, acid reception through the olfactory system in moths have been hardly tackled, and few studies can be found on cellular responding patterns.

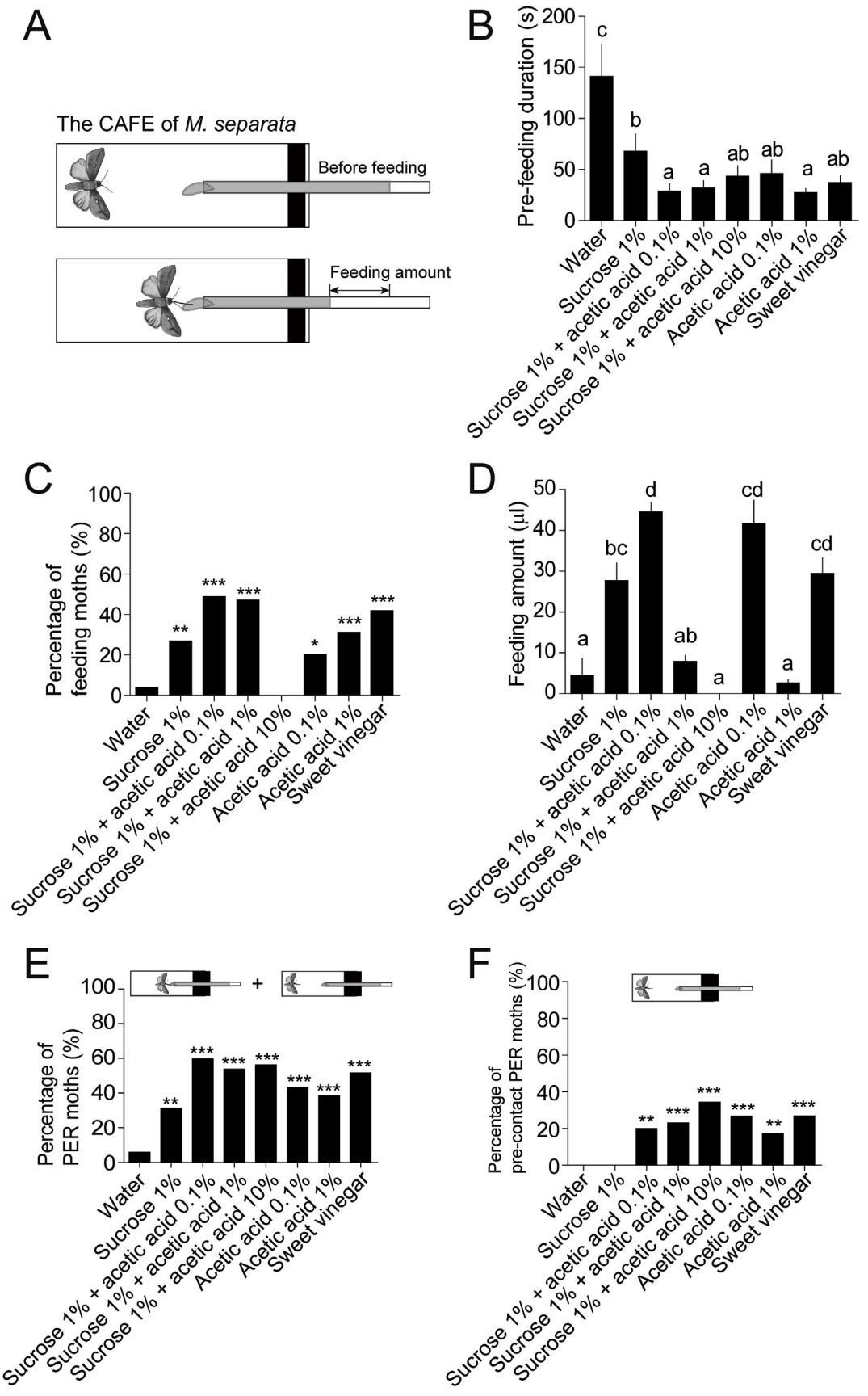

(caption on next page)

Fig. 5. Behavioral responses of female *M. separata* to acetic acid in the CAFE assay. (A) Schematic diagram of the experimental setup. (B) The pre-feeding duration of 12 h fasted moths. The sweet vinegar solution containing 1% acetic acid was used. Different lower-case letters indicate significant differences among treatments ($F_{7, 86} = 5.7$, $P < 0.0001$). Error bars indicate + s.e.m. **(C)** The percentage of feeding moths. Asterisks indicate significant higher percentages of the treatments comparing with water (*: $P < 0.05$, **: $P < 0.01$, ***: $P < 0.001$). 0.1% acetic acid +1% sucrose was significantly higher than 1% sucrose alone ($P = 0.044$). (D)The feeding amount in the first meal of moths. Different lower-case letters indicate significant differences among treatments ($F_{6, 67} = 20.5$, $P < 0.0001$). Error bars indicate + s.e.m. (E) The percentage of PER moths. Asterisks indicate significant higher percentages of the treatments comparing with water (***: $P < 0.001$). PERs induced by 0.1%, 1%, and 10% acetic acid +1% sucrose and the sweet vinegar solution were significantly higher than that by 1% sucrose alone (0.1%: $P = 0.014$, 1%: $P = 0.049$, 10%: $P = 0.038$, sweet vinegar: $P = 0.046$). (F) The percentage of pre-contact PER moths. Asterisks indicate significant higher percentages of the treatments comparing with water and 1% sucrose (**: $P < 0.01$, ***: $P < 0.001$).

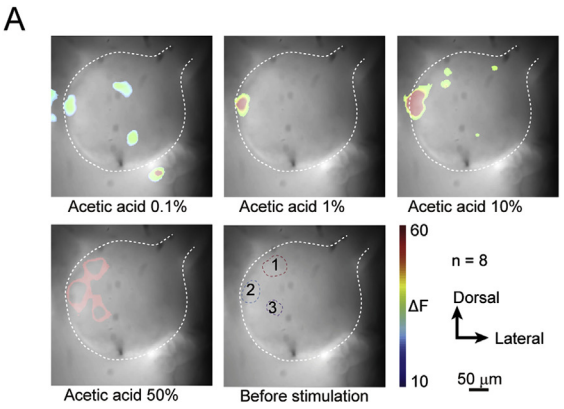

Fig. 6. Response activities of antennal lobes to acetic acid in *M. separata* females. (A) Representative evoking patterns of antennal lobes by acetic acid dosages. Color circles indicate areas of interest. **(B)** Dosage response activities in ROI2 to acetic acid. Dots with different lower-case letters indicate significant differences of *ΔF/F0* values among dosages ($F_{5, 102} = 24.7$, $P < 0.0001$). Error bars indicate ± s.e.m.

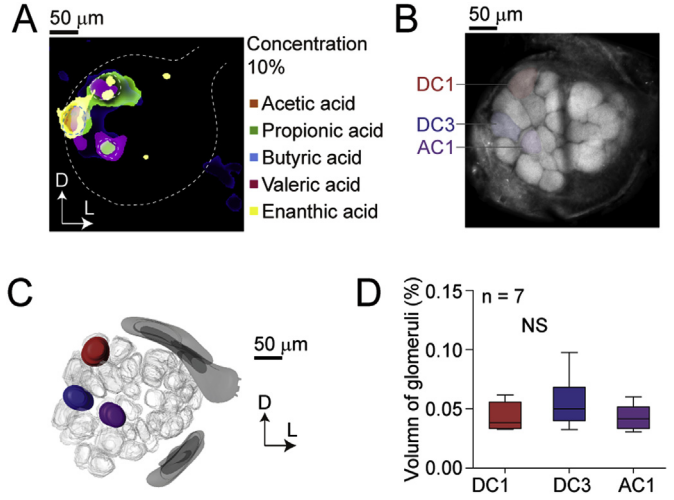

Fig. 7. Identification of acid evoking glomeruli in *M. separata* females. (A) Merged evoking areas from top 5 active acids. **(B)** Antennal lobe atlas of female adults. The three glomeruli were named according to locations as DC1 (dorsal central 1), DC3, and AC1 (anterior central 1), respectively. **(C)** Re-construction of 3-D model of the female antennal lobe using the data from (B). Colored glomeruli showing conserved positions for DC1 (red), DC3 (blue), and AC1 (purple) glomeruli in females. **(D)** The volume comparison of three glomeruli ($F_{2, 18} = 1.26$, $P = 0.308$). Error bars indicate 95% c.i.

The identified DC1 and DC3 glomeruli in *M. separata* have some anatomic similarities with the recently reported acid sensing G22 and G23 glomeruli in *Manduca sexta* (Bisch-Knaden et al., 2018), which may help future works on acid signal processing and integration in antennal lobes. In fact, it was observed that anatomically similar glomeruli could share the same behavioral decision pathways in different *Drosophila* species (Auer et al., 2019; Prieto-Godino et al., 2017).

The vinegar fly, *D. melanogaster*, has shown its preference to acidity medium in order to exhibit foraging (Zhu et al., 2003), mating (Lebreton et al., 2012), and oviposition (Chen and Amrein, 2017). The coding process for acid attractiveness to *Drosophila* involves both olfaction and gustation. Initial orientation behaviors are decided via olfactory sensing through antennal IRs that deliver distinct evoking patterns in the antennal lobes (Prieto-Godino et al., 2016, 2017). After approaching, successive behaviors including feeding, oviposition, or ingesting can also be governed by IRs which housed in the taste organs through gustatory receptor neuron signaling (Chen and Amrein, 2017). Nevertheless, the central decision mechanisms on gustation mediated acid attractiveness in *Drosophila* still need to be discovered. For moth species like *M. sexta*, acids elicited distinct areas of glomeruli which related to either feeding or oviposition attempts (Bisch-Knaden et al., 2018). Our work revealed the importance of acetic acid in the food selection of *M. separata*. The feeding status-dependent behaviors and dedicated glomeruli evoking patterns we observed in *M. separata* may be the common features on acetic acid perception across insect species (Zhu et al., 2003; Semmelhack and Wang, 2009; Bisch-Knaden et al., 2018).

The studies on molecular bases of olfactory sensing to acids in *Drosophila* have made important progress recently. The *DmelIr8a* has been reported as an essential co-receptor for acid sensing (Abuin et al., 2011; Ai et al., 2010; Benton et al., 2009). A tetramer complex formed by four monomeric structures (*DmelIr8a* + *DmelIrx/DmelIrx*) from two or three IRs is needed to perform olfactory responsiveness (Abuin et al., 2011, 2019; Ai et al., 2013). Among the identified *DmelIRs*, *DmelIr64a* expressing neurons are necessary and sufficient for *D. melanogaster* to avoid 5% of acetic acid and other acids including propionic acid, butyric acid, isobutyric acid, and hexanoic acid (Ai et al., 2010). *DmelIr75a* encodes an acetic acid receptor in *D. melanogaster*, but its ortholog *DsecIr75a* in *D. sechellia* as a transcribed pseudogene is tuned broadly to butyric acid, propionic acid, 2-oxo-pentanoic acid, and acetic acid (Rytz et al., 2013; Joseph and Carlson, 2015; Prieto-Godino et al., 2016). DmelIR75b is mainly tuned to butyric acid and propionic acid, while DsecIR75b is mainly tuned to hexanoic acid which is a key host odor mediated attractiveness of *D. sechellia*. A single residue change results in the functional shift between DmelIR75b and DsecIR75b (Prieto-Godino et al., 2017). DmelIR75c and DsecIR75c have very similar responding pattern to propionic acid, butyric acid, and 2-oxo-pentanoic acid (Prieto-Godino et al., 2017). However, the molecular basis of acetic acid attractiveness in *D. melanogaster* is still unclear. In this study, we identify the full length cDNAs of *MsepIr8a*, *MsepIr64a*, *MsepIr75q1* and *MsepIr75q2*. MsepIR8a and DmelIR8a sharing 49.10% amino acid identity are highly conserved in LBD and trans-membrane

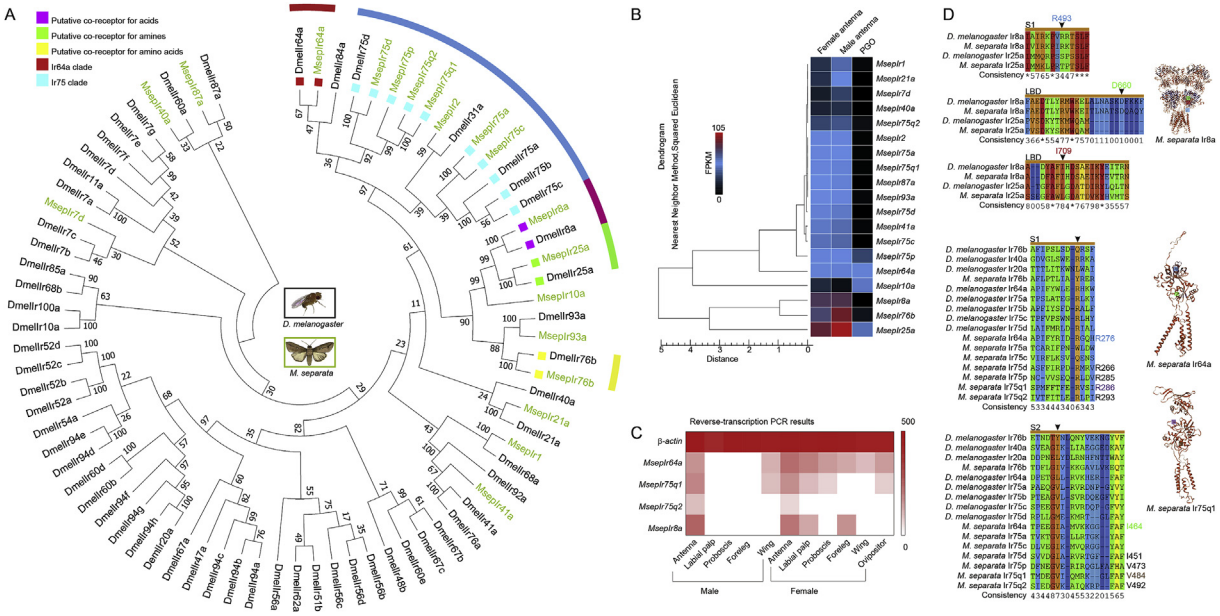

Fig. 8. Screening of putative acetic acid sensing IRs in *M. separata*. (A) Phylogenetic analysis of related IRs from multiple species. Deposited *Ir* gene information was listed in Table S3. The evolutionary history was inferred using the Neighbor-Joining method. The optimal tree with the sum of branch length = 57.33489162 is shown. The evolutionary distances were computed using the Poisson correction method and are in the units of the number of amino acid substitutions per site. This analysis involved 78 amino acid sequences. All ambiguous positions were removed for each sequence pair (pairwise deletion option). There were a total of 1414 positions in the final dataset. **(B)** Expression profiles of 19 *M. separata Irs* in transcriptome of female antennae, male antennae, and PGO (pheromone gland and ovipositor), respectively. **(C)** Tissue expression of *Irs* by RT-PCR using cDNAs from different body parts of *M. separata*. *β-actin* was used as reference. **(D)** Structural prediction and alignment of selected *M. separata* IRs. Arrows indicate key amino acid residues.

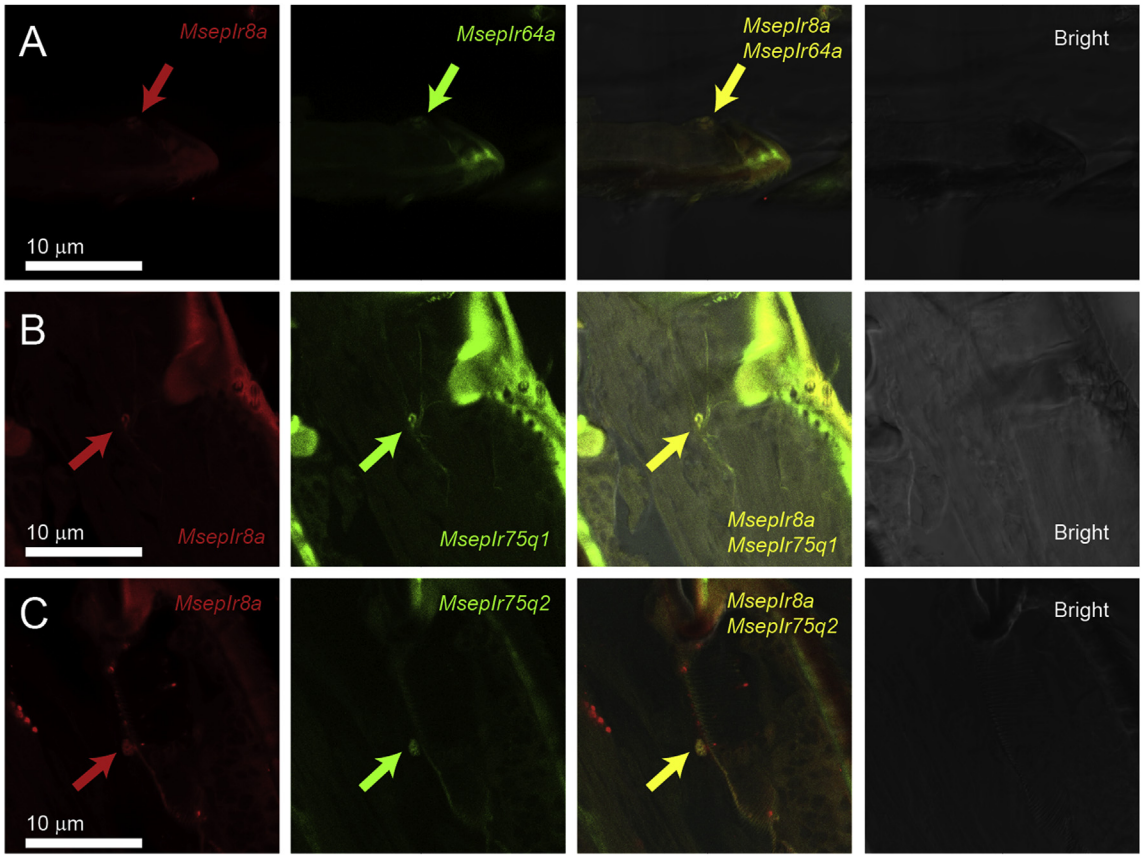

Fig. 9. Localizations of *Ir8a*, *Ir64a*, *Ir75q1*, and *Ir75q2* in antennae of female *M. separata* adults. (A–C) Co-expression patterns of *Ir8a*, *Ir64a*, *Ir75q1*, and *Ir75q2* in *M. separata* female antennae. Arrows show labelled somata with probes synthesized from targeted genes. Digoxin (red) and biotin (green) were used to label the two genes respectively in each pair.

region (aa 373–834 of MsepIR8a) with up to 71.49% amino acid identity. According to this structural similarity and also FISH test results, we suggest that MsepIR8a is most likely to be the acid sensing IR co-receptor in *M. separata*. For other IRs, MsepIR64a has 30.32% amino acid identity with DmelIR64a; MsepIR75q1 and MsepIR75q2 have 25.51% and 22.76% identities with DmelIR75a, respectively. Although the identities are low, they are already the highest ones when comparing with all the *D. drosophila* IRs. The further deorphanization of acetic acid sensing IRs in *M. separata* could express the combinations of each of these *IR* genes with *MsepIr8a* in heterologous expression systems, such as the *Xenopus* oocytes and the *Drosophila Or22a* empty neuron system, both of which are already proved to have well worked on IR functional characterization (Dascal, 2008; Ai et al., 2013; Abuin et al., 2011). Meanwhile, genetic tools such as the *CRISPR-Cas9* system can also be introduced to explore related neuron circuits and behavioral consequences of candidate IRs.

Last but not least, enanthic acid stimulated robust responsiveness in as1, indicating that it was the best ligand among tested chemicals for IR pathway at periphery. However, this acid did not evoke high response of DC3, and later could not attract the moths. In *Drosophila*, non-linearized transmission of olfactory signals exists among peripheral inputs/outputs and central brain levels due to many architectural variances (Bhandawat et al., 2007; Caron et al., 2013; Chou et al., 2010; Grabe et al., 2016), and peripheral coding patterns sometimes are not sufficient enough to deliver behavioral outputs (Choo et al., 2018). The similar coding mechanism may also exist in *M. separata*, which delivers different behavioral outputs of the moth to acetic acid and other acids including enanthic acid. To date, few studies have been conducted on enanthic acid (Urbanek et al., 2012; Watanabe et al., 2012), and neither of the studies have discovered ecological significance of this component in insects. However, we don't exclude the possible involvement of enanthic acid in mating or oviposition.

Author contributions

CZW conceived the project. RT and CZW designed the study. RT conducted electrophysiological, cellular, and molecular tests. RT, LQH, and NJJ conducted bioassays. NJJ, CN, GCL, and RT conducted antennae transcriptome sequencing and data analysis. RT and CZW analyzed data and wrote the manuscript.

Declaration of competing interest

The authors declare that they have no competing interests.

Ethics

No human or animal subjects were involved within the current research.

Acknowledgements

This work was supported by National Natural Science Foundation of China (grant number 31830088) and National Key R&D Program of China (Grant number 2017YFD0200400). Funding bodies of the study had no role in the design of the study, collection, analysis, interpretation of data, or in writing the manuscript. We thank Prof. Feng Zhang and MARA-CABI Joint Laboratory for Bio-safety, IPP-CAAS for supporting Rui Tang's research works in IOZ-CAS. We thank Prof. Chuan Zhou for providing devices for the moth CAFE assay. We thank Prof. Giovanni Galizia for helping with optical imaging data analysis. We thank Dr. Hao Guo, Dr. Stefan Toepfer and Prof. Fang-Hao Wan for the valuable comments on the manuscript. We thank Rui Wang, Xiao-Wei Qin and Lin Yang from the State Key Laboratory for their assistance with chemical analysis and *in situ* hybridization; Dr. Meng Xu, Dr. Wu Han, Yan Chen and Dr. Ke Yang for technical assistance in the SSR, calcium imaging, and molecular biology experiments, respectively. We also thank Dr. Jin-Ping Zhang, Dr. Ya-Lan Sun and Dr. Xiao-Jing Jiang for providing insects for GC-EAD tests, B. F. A. Xiao-Qian Bao for technical support with insect graph development, Dr. Yi-Nan Fang for the technical support with the Matlab clustering analysis.

Appendix A. Supplementary data

Supplementary data related to this article can be found at https://doi.org/10.1016/j.ibmb.2019.103312.

References

Abuin, L., Bargeton, B., Ulbrich, M.H., Isacoff, E.Y., Kellenberger, S., Benton, R., 2011. Functional architecture of olfactory ionotropic glutamate receptors. Neuron 69 (1), 44–60. https://doi.org/10.1016/j.neuron.2010.11.042.

Abuin, L., Prieto-Godino, L.L., Pan, H., Gutierrez, C., Huang, L., Jin, R., et al., 2019. *In vivo* assembly and trafficking of olfactory Ionotropic Receptors. BMC Biol. 17 (1), 34.

Ahn, J.E., Chen, Y., Amrein, H., 2017. Molecular basis of fatty acid taste in *Drosophila*. eLife 6, e30115.

Ai, M., Min, S., Grosjean, Y., Leblanc, C., Bell, R., Benton, R., et al., 2010. Acid sensing by the *Drosophila* olfactory system. Nature 468 (7324), 691–695. https://doi.org/10.1038/nature09537.

Ai, M., Blais, S., Park, J.Y., Min, S., Neubert, T.A., Suh, G.S., 2013. Ionotropic glutamate receptors *IR64a* and *IR8a* form a functional odorant receptor complex *in vivo* in *Drosophila*. J. Neurosci. 33 (26), 10741–10749. https://doi.org/10.1523/JNEUROSCI.5419-12.2013.

Allmann, S., Spathe, A., Bisch-Knaden, S., Kallenbach, M., Reinecke, A., Sachse, S., et al., 2013. Feeding-induced rearrangement of green leaf volatiles reduces moth oviposition. eLife 2, e00421. https://doi.org/10.7554/eLife.00421.

Auer, T.O., Khallaf, M.A., Silbering, A.F., Zappia, G., Ellis, K., et al., 2019. The making of an olfactory specialist. BioRxiv 546507. https://doi.org/10.1101/546507.

Benton, R., Vannice, K.S., Gomez-Diaz, C., Vosshall, L.B., 2009. Variant ionotropic glutamate receptors as chemosensory receptors in *Drosophila*. Cell 136 (1), 149–162. https://doi.org/10.1016/j.cell.2008.12.001.

Berg, B.G., Galizia, C.G., Brandt, R., Mustaparta, H., 2002. Digital atlases of the antennal lobe in two species of tobacco budworm moths, the Oriental *Helicoverpa assulta* (male) and the American *Heliothis virescens* (male and female). J. Comp. Neurol. 446 (2), 123–134. https://doi.org/10.1002/cne.10180.

Bhandawat, V., Olsen, S.R., Gouwens, N.W., Schlief, M.L., Wilson, R.I., 2007. Sensory processing in the *Drosophila* antennal lobe increases reliability and separability of ensemble odor representations. Nat. Neurosci. 10 (11), 1474–1482. https://doi.org/10.1038/nn1976.

Bisch-Knaden, S., Dahake, A., Sachse, S., Knaden, M., Hansson, B.S., 2018. Spatial representation of feeding and oviposition odors in the brain of a hawkmoth. Cell Rep. 22 (9), 2482–2492. https://doi.org/10.1016/j.celrep.2018.01.082.

Caron, S.J., Ruta, V., Abbott, L.F., Axel, R., 2013. Random convergence of olfactory inputs in the *Drosophila* mushroom body. Nature 497 (7447), 113–117. https://doi.org/10.1038/nature12063.

Cha, D.H., Adams, T., Rogg, H., Landolt, P.J., 2012. Identification and field evaluation of fermentation volatiles from wine and vinegar that mediate attraction of spotted wing *Drosophila, Drosophila suzukii*. J. Chem. Ecol. 38 (11), 1419–1431. https://doi.org/10.1007/s10886-012-0196-5.

Chen, Y., Amrein, H., 2017. Ionotropic receptors mediate drosophila oviposition preference through sour gustatory receptor neurons. Curr. Biol. 27, 1–10. https://doi.org/10.1016/j.cub.2017.08.003.

Chiu, W.F., 1982. Advances of science of plant protection in the people's Republic of China. Annu. Rev. Phytopathol. 20, 71–92. https://doi.org/10.1146/annurev.py.20.090182.000443.

Choo, Y.M., Xu, P., Hwang, J.K., Zeng, F., Tan, K., Bhagavathy, G., et al., 2018. Reverse chemical ecology approach for the identification of an oviposition attractant for *Culex quinquefasciatus*. Proc. Natl. Acad. Sci. U.S.A. 115 (4), 714–719. https://doi.org/10.1073/pnas.1718284115.

Chou, Y.H., Spletter, M.L., Yaksi, E., Leong, J.C., Wilson, R.I., Luo, L., 2010. Diversity and wiring variability of olfactory local interneurons in the *Drosophila* antennal lobe. Nat. Neurosci. 13 (4), 439–449. https://doi.org/10.1038/nn.2489.

Dascal, N., 2008. The use of *Xenopus* oocytes for the study of ion channel. Crit. Rev. Biochem. 22 (4), 317–387. https://doi.org/10.3109/10409238709086960.

de Bruyne, M., Foster, K., Carlson, J.R., 2001. Odor coding in the *Drosophila* antenna. Neuron 30 (2), 537–552. https://doi.org/10.1016/S0896-6273(01)00289-6.

Dweck, H.K., Ebrahim, S.A., Thoma, M., Mohamed, A.A., Keesey, I.W., Trona, F., et al., 2015. Pheromones mediating copulation and attraction in *Drosophila*. Proc. Natl. Acad. Sci. U.S.A. 112 (21), E2829–E2835. https://doi.org/10.1073/pnas.1504527112.

Ebrahim, S.A., Dweck, H.K., Stokl, J., Hofferberth, J.E., Trona, F., Weniger, K., et al., 2015. *Drosophila* avoids parasitoids by sensing their semiochemicals via a dedicated olfactory circuit. PLoS Biol. 13 (12), e1002318. https://doi.org/10.1371/journal.pbio.1002318.

Enjin, A., Zaharieva, E.E., Frank, D.D., Mansourian, S., Suh, G.S.B., Gallio, M., et al., 2016. Humidity sensing in *Drosophila*. Curr. Biol. 26 (10), 1352–1358. https://doi.org/10.1016/j.cub.2016.03.049.

Faucher, C.P., Hilker, M., de Bruyne, M., 2013. Interactions of carbon dioxide and food

odours in *Drosophila*: olfactory hedonics and sensory neuron properties. PLoS One 8 (2), e56361. https://doi.org/10.1371/journal.pone.0056361.
Ganguly, A., Pang, L., Duong, V.K., Lee, A., Schoniger, H., Varady, E., et al., 2017. A molecular and cellular context-dependent role for *Ir76b* in detection of amino acid taste. Cell Rep. 18 (3), 737–750. https://doi.org/10.1016/j.celrep.2016.12.071.
Ghaninia, M., Olsson, S.B., Hansson, B.S., 2014. Physiological organization and topographic mapping of the antennal olfactory sensory neurons in female hawkmoths. *Manduca sexta*. Chem. Senses 39, 655–671. https://doi.org/10.1093/chemse/bju037.
Gorter, J.A., Jagadeesh, S., Gahr, C., Boonekamp, J.J., Levine, J.D., Billeter, J.C., 2016. The nutritional and hedonic value of food modulate sexual receptivity in *Drosophila melanogaster* females. Sci. Rep. 6, 19441. https://doi.org/10.1038/srep19441.
Gou, B., Liu, Y., Guntur, A.R., Stern, U., Yang, C.H., 2014. Mechanosensitive neurons on the internal reproductive tract contribute to egg-laying-induced acetic acid attraction in *Drosophila*. Cell Rep. 9 (2), 522–530. https://doi.org/10.1016/j.celrep.2014.09.033.
Grabe, V., Baschwitz, A., Dweck, H.K.M., Lavista-Llanos, S., Hansson, B.S., 2016. Sachse S. Elucidating the neuronal architecture of olfactory glomeruli in the *Drosophila* antennal lobe. Cell Rep. 16 (12), 3401–3413. https://doi.org/10.1016/j.celrep.2016.08.063.
Haas, B.J., Papanicolaou, A., Yassour, M., Grabherr, M., Blood, P.D., Bowden, J., et al., 2013. *De novo* transcript sequence reconstruction from RNA-seq using the Trinity platform for reference generation and analysis. Nat. Protoc. 8 (8), 1494–1512. https://doi.org/10.1038/nprot.2013.084.
Hussain, A., Zhang, M., Ucpunar, H.K., Svensson, T., Quillery, E., Gompel, N., et al., 2016. Ionotropic chemosensory receptors mediate the taste and smell of polyamines. PLoS Biol. 14 (5), e1002454. https://doi.org/10.1371/journal.pbio.1002454.
Jiang, X.F., Zhang, L., Cheng, Y.X., Luo, L.Z., 2014. Current status and trends in research on the oriental armyworm, *Mythimna separata* (Walker) in China. Chin. J. Appl. Entomol. 51 (4), 881–889. https://doi.org/10.7679/j.issn.2095?1353.2014.108.
Joseph, R.M., Carlson, J.R., 2015. *Drosophila* chemoreceptors: a molecular interface between the chemical world and the brain. Trends Genet. 31 (12), 683–695. https://doi.org/10.1016/j.tig.2015.09.005. Epub 2015/10/20.
Joseph, R.M., Devineni, A.V., King, I.F., Heberlein, U., 2009. Oviposition preference for and positional avoidance of acetic acid provide a model for competing behavioral drives in *Drosophila*. Proc. Natl. Acad. Sci. U.S.A. 106 (27), 11352–11357. https://doi.org/10.1073/pnas.0901419106.
Knecht, Z.A., Silbering, A.F., Ni, L., Klein, M., Budelli, G., Bell, R., et al., 2016. Distinct combinations of variant ionotropic glutamate receptors mediate thermosensation and hygrosensation in *Drosophila*. eLife, e17879. https://doi.org/10.1101/056267.
Ko, K., Root, M.C., Lindsay, A.S., Zaninovich, A.O., Shepherd, K.A., Wasserman, A.S., et al., 2015. Starvation promotes concerted modulation of appetitive olfactory behavior via parallel neuromodulatory circuits. eLife 4, e08298. https://doi.org/10.7554/eLife.08298.002.
Koh, T.W., He, Z., Gorur-Shandilya, S., Menuz, K., Larter, N.K., Stewart, S., et al., 2014. The *Drosophila IR20a* clade of ionotropic receptors are candidate taste and pheromone receptors. Neuron 83 (4), 850–865. https://doi.org/10.1016/j.neuron.2014.07.012.
Kumar, S., Stecher, G., Tamura, K., 2016. MEGA7: molecular evolutionary genetics analysis version 7.0 for bigger datasets. Mol. Biol. Evol. 33 (7), 1870–1874. https://doi.org/10.1093/molbev/msw054.
Landolt, P., Zhang, Q.H., 2016. Discovery and development of chemical attractants used to trap pestiferous social wasps (Hymenoptera: Vespidae). J. Chem. Ecol. 42 (7), 655–665. https://doi.org/10.1007/s10886-016-0721-z.
Lebreton, S., Becher, P.G., Hansson, B.S., Witzgall, P., 2012. Attraction of *Drosophila melanogaster* males to food-related and fly odours. J. Insect Physiol. 58 (1), 125–129. https://doi.org/10.1016/j.jinsphys.2011.10.009.
Lee, Y., Poudel, S., Kim, Y., Thakur, D., Montell, C., 2018. Calcium taste avoidance in *Drosophila*. Neuron 97 (1), 67–74. https://doi.org/10.1016/j.neuron.2017.11.038.
Lofaldli, B.B., Kvello, P., Mustaparta, H., 2010. Integration of the antennal lobe glomeruli and three projection neurons in the standard brain atlas of the moth *Heliothis virescens*. Front. Syst. Neurosci. 4, 5. https://doi.org/10.3389/neuro.06.005.2010.
MacQueen, J., 1967. Some methods for classification and analysis of multivariate observations. 1967 In: Proceedings of the fifth Berkeley symposium on mathematical statistics and probability. 1. pp. 281–297 14.
Meagher, R.L., Mislevy, P., 2005. Trapping Mocis spp. (Lepidoptera: Noctuidae) adults with different attractants. Fla. Entomol. 88 (4), 424–430. https://doi.org/10.1653/0015-4040(2005)88[424:Tmslna]2.0.Co;2.
Münch, D., Galizia, C.G., 2016. DoOR 2.0-comprehensive mapping of *Drosophila melanogaster* odorant responses. Sci. Rep. 6, 21841. https://doi.org/10.1038/srep21841.
Ni, L., Klein, M., Svec, K., Budelli, G., Chang, E.C., Benton, R., et al., 2016. The ionotropic receptors *IR21a* and *IR25a* mediate cool sensing in *Drosophila*. eLife, e13254. https://doi.org/10.1101/032540.
Ning, C., Yang, K., Xu, M., Huang, L.Q., Wang, C.Z., 2016. Functional validation of the carbon dioxide receptor in labial palps of *Helicoverpa armigera* moths. Insect Biochem. Mol. Biol. 73, 12–19. https://doi.org/10.1016/j.ibmb.2016.04.002.
Penniston, K.L., Nakada, S.Y., Holmes, R.P., Assimos, D.G., 2008. Quantitative assessment of citric acid in lemon juice, lime juice, and commercially-available fruit juice products. J. Endourol. 22 (3), 567–570. https://doi.org/10.1089/end.2007.0304.
Prieto-Godino, L.L., Rytz, R., Bargeton, B., Abuin, L., Arguello, J.R., Peraro, M.D., et al., 2016. Olfactory receptor pseudo-pseudogenes. Nature 539 (7627), 93–97. https://doi.org/10.1038/nature19824.
Prieto-Godino, L.L., Rytz, R., Cruchet, S., Bargeton, B., Abuin, L., Silbering, A.F., et al., 2017. Evolution of acid-sensing olfactory circuits in Drosophilids. Neuron 93 (3), 661–676. https://doi.org/10.1016/j.neuron.2016.12.024. e6.
Raji, J.I., Melo, N., Castillo, J.S., Gonzalez, S., Saldana, V., Stensmyr, M.C., DeGennaro, M., 2019. *Aedes aegypti* mosquitoes detect acidic volatiles found in human odor using the IR8a pathway. Curr. Biol. 29, 1253–1262. https://doi.org/10.1016/j.cub.2019.02.045.
Rimal, S., Sang, J., Poudel, S., Thakur, D., Montell, C., Lee, Y., 2019. Mechanism of acetic acid gustatory repulsion in *Drosophila*. Cell Rep. 26 (6), 1432–1442. https://doi.org/10.1016/j.celrep.2019.01.042.
Rousseeuw, P.J., 1987. Silhouettes: a graphical aid to the interpretation and validation of cluster analysis. J. Comput. Appl. Math. 20 (20), 53–65. https://doi.org/10.1016/0377-0427(87)90125-7.
Rytz, R., Croset, V., Benton, R., 2013. Ionotropic receptors (IRs): chemosensory ionotropic glutamate receptors in *Drosophila* and beyond. Insect Biochem. Mol. Biol. 43 (9), 888–897. https://doi.org/10.1016/j.ibmb.2013.02.007.
Saitou, N., Nei, M., 1987. The Neighbor-joining method: a new method for reconstructing phylogenetic trees. Mol. Biol. Evol. 4 (4), 406–425. https://doi.org/10.1093/oxfordjournals.molbev.a040454.
Sánchez-Alcañiz, J.A., Silbering, A.F., Croset, V., Zappia, G., Sivasubramaniam, A.K., Abuin, L., et al., 2018. An expression atlas of variant ionotropic glutamate receptors identifies a molecular basis of carbonation sensing. Nat. Commun. 9 (1), 4252. https://doi.org/10.1038/s41467-018-06453-1.
Semmelhack, J.L., Wang, J.W., 2009. Select *Drosophila* glomeruli mediate innate olfactory attraction and aversion. Nature 459 (7244), 218–223. https://doi.org/10.1038/nature07983.
Tang, R., Zhang, J.P., Zhang, Z.N., 2012. Electrophysiological and behavioral responses of male fall webworm moths (*Hyphantria cunea*) to herbivory-induced mulberry (*Morus alba*) leaf volatiles. PLoS One 7 (11), e49256. https://doi.org/10.1371/journal.pone.0049256.
Tang, R., Zhang, F., Kone, N.G., Chen, J.H., Zhu, F., Han, R.C., et al., 2016. Identification and testing of oviposition attractant chemical compounds for *Musca domestica*. Sci. Rep. 6, 33017. https://doi.org/10.1038/srep33017.
Toth, M., Szarukan, I., Dorogi, B., Gulyas, A., Nagy, P., Rozgonyi, Z., 2010. Male and female noctuid moths attracted to synthetic lures in Europe. J. Chem. Ecol. 36 (6), 592–598. https://doi.org/10.1007/s10886-010-9789-z.
Urbanek, A., Szadziewski, R., Stepnowski, P., Boros-Majewska, J., Gabriel, I., Dawgul, M., et al., 2012. Composition and antimicrobial activity of fatty acids detected in the hygroscopic secretion collected from the secretory setae of larvae of the biting midge *Forcipomyia nigra* (Diptera: Ceratopogonidae). J. Insect Physiol. 58 (9), 1265–1276. https://doi.org/10.1016/j.jinsphys.2012.06.014.
Watanabe, H., Ai, H., Yokohari, F., 2012. Spatio-temporal activity patterns of odor-induced synchronized potentials revealed by voltage-sensitive dye imaging and intracellular recording in the antennal lobe of the cockroach. Front. Syst. Neurosci. 6 (55), 1–18. https://doi.org/10.3389/fnsys.2012.00055.
Wu, H., Xu, M., Hou, C., Huang, L.Q., Dong, J.F., Wang, C.Z., 2015. Specific olfactory neurons and glomeruli are associated to differences in behavioral responses to pheromone components between two *Helicoverpa* species. Front. Behav. Neurosci. 9, 206. https://doi.org/10.3389/fnbeh.2015.00206.
Xu, M., Guo, H., Hou, C., Wu, H., Huang, L.Q., Wang, C.Z., 2016. Olfactory perception and behavioral effects of sex pheromone gland components in *Helicoverpa armigera* and *Helicoverpa assulta*. Sci. Rep. 6, 22998. https://doi.org/10.1038/srep22998.
Zhao, X.C., Chen, Q.Y., Guo, P., Xie, G.Y., Tang, Q.B., Guo, X.R., et al., 2016. Glomerular identification in the antennal lobe of the male moth *Helicoverpa armigera*. J. Comp. Neurol. 524 (15), 2993–3013. https://doi.org/10.1002/cne.24003.
Zhu, J., Park, K.C., Baker, T.C., 2003. Identification of odors from overripe mango that attract vinegar flies, *Drosophila melanogaster*. J. Chem. Ecol. 29 (4), 899–909. https://doi.org/10.1023/a:1022931816351.